IEEE Access
Multidisciplinary | Rapid Review | Open Access Journal

Received 3 August 2023, accepted 25 September 2023, date of publication 30 October 2023,
date of current version 6 November 2023.

Digital Object Identifier 10.1109/ACCESS.2023.3328583

RESEARCH ARTICLE

Experimental Investigation of 5G Base Station Functionalities in Reverberation Chamber at Millimeter-Wave

MICHELE COLOMBO[1], RICCARDO DIAMANTI[2], LUCA BASTIANELLI[3,4], (Member, IEEE), GABRIELE GRADONI[5,6], (Member, IEEE), EMANUEL COLELLA[3,4], VALTER MARIANI PRIMIANI[3,4], (Senior Member, IEEE), FRANCO MOGLIE[3,4], (Senior Member, IEEE), AND DAVIDE MICHELI[7]

[1]Nokia Networks Italia, 20871 Vimercate, Italy
[2]TIM S.p.A., 60131 Ancona, Italy
[3]Dipartimento di Ingegneria dell'Informazione, Università Politecnica delle Marche, 60131 Ancona, Italy
[4]Consorzio Nazionale Interuniversitario per le Telecomunicazioni (CNIT), 43124 Parma, Italy
[5]Institute for Communication Systems (ICS), University of Surrey, GU2 7XH Guildford, U.K.
[6]Department of Computer Science and Technology, University of Cambridge, CB3 0FD Cambridge, U.K.
[7]TIM S.p.A., 00189 Rome, Italy

Corresponding author: Luca Bastianelli (l.bastianelli@pm.univpm.it)

This work was supported by the European Union (EU) HORIZON 2020 (H2020) Reconfigurable Intelligent Sustainable Environments for 6G Wireless Networks (RISE-6G) Project under Grant 101017011.

ABSTRACT The performance and functionalities of a commercial fifth generation base station are evaluated inside the reverberation chamber at the mmWave frequency range. The base station capability to operates in different propagation environment conditions reproduced by the reverberation chamber is investigated. Throughput, modulation code scheme and beamforming are analyzed for different real life scenarios both in uplink and downlink. Experimental results inform network operators in their evaluation of the base station operation: i) in many scenarios within a laboratory; ii) in the assessment of whether expected benefit justifies the additional costs in an operating actual network.

INDEX TERMS 5G, base station, mmWave, reverberation chamber, key-performance indicators, live radio access network, throughput, RSRP, beamforming.

I. INTRODUCTION

Mobile communication has rapidly increased over last years, evolving from only voice services to dense interconnected environment serving multiple services. Those services run on a system based on the same infrastructure that is able to support a large number of applications. The system provides connection among a massive number of devices ensuring low latency and high-speed communication, such as autonomous vehicles scenarios, smart cities and so on. In the next few years, it is forecast that the data traffic and services will enormously increase, the 5G represents not only a solution but the revolution we need. The 5G wireless technology is a significant advancement over previous generations. It solves all prior disadvantages, such as a lack of coverage, lack of performance at cell edges, and dropped calls. In wireless applications the propagation environment may arise some problems in the overall system operation. Some techniques can be adopted in the 5G system in order to mitigate and improve the connectivity. In particular, BSs will be equipped by massive MIMO antennas which provide eMBB to be leveraged for many applications. The 5G technology introduces novelty and its application will revolutionize many areas, such as smart city, IoT, M2M communication, health care and we can go on for much longer listing the most varied applications [1], [2], [3]. In the not-too-distant future, as early as five years from now, it is expected a huge increment of mobile traffic [4], [5], [6]. Mobile operators are in a race to deploy technologies in order to support networks with a massive number of devices, interconnected

The associate editor coordinating the review of this manuscript and approving it for publication was P. Venkata Krishna.

each others able leverage high bandwidth in particular at the mmWave frequency range, such as 1 Gbps or more. On the one hand mobile operators have the possibility to virtualize and slicing network in order to support different product/services. On the other hand, wireless networks can be integrated with passive/active devices able to improve the radio communication and they enable functionalities taking advantage of mobile edge computing. Those devices are RISs which can be adopted for smart and programmable radio environments, thus by giving new opportunities and new paradigms [7], [8], [9]. From the mobile operator point of view, the perspective of reducing: the transmitting power, interference, electromagnetic field exposure [10], [11] to non-intended user and so on, makes the technology very appealing. Beyond the current frequency bands, mobile operators are going to occupy the mmWave frequency bands [12], [13] that guarantee a part of spectrum which is not fully licensed. This spectrum allows to support a high data rate and large number of interconnections. On the contrary, mmWave band exhibits a large path loss, in particular when the signal encounters an obstacle. To overcome this issue mobile operator has different options such as the adoption of smart antennas, a mix of transmission techniques or either the option to be discarded i.e. the increase in transmitted power. In order to perform measurements with a commercial Nokia 5G BS, equipped by a smart antenna with beamforming, we take advantage of the characteristics of the RC [14], [15]. The RC can be efficiently adopted to carry out measurements of total radiated power of general electronic equipment [16] and recently applied to base station radiated power determination [17]. It is interesting to note that the RC methodology is applicable to the higher 5G frequencies too, which are 28 and 39 GHz and regardless of beamforming technology [18]. The method has been also investigated in terms of associated uncertainty [19] affected by the coherence bandwidth due to the large bandwidth adopted by modern communication systems. The availability of a very rich multipath environment like an RC is useful to carry out complete OTA on wireless systems [20] because real life propagation conditions can be reproduced. The RC is an electrically large cavity where the electromagnetic field is statistically uniform, isotropic and randomly polarized within a defined region, called working volume [21], [22]. The whole surface of the RC is covered by metal. The RC is equipped by stirrers that continuously rotate in order to mix the electromagnetic field and thus to replicate dynamic propagation conditions [23].

The RC is a richly multipath environment that does not represent the majority of real life scenarios, but by adding absorbing materials the RC load increases and the corresponding time delay spread progressively decreases thus allowing us to use it for wireless tests. The presence of absorbing panels reduces reflected signals and we are able to control the multipath richness in order to emulate the desired real life propagation environments [24], [25], [26]. By properly setting the RC loading, time delay spread reaches typically values encountered in real life environments. In particular, to this purpose we can consider few parameters, such as the PDP and time delay spread (τ), the Q-factor and the Rician K-factor. Those values are tuned by varying the number of absorbing panels, planar and/or pyramidal. The time delay spread is an indication of the spread affecting the signal components, as they are coming to the receiver. The decay time denotes the time after which the reflected component is negligible and it directly influences the coherence time. Finally, the Q-factor is the capability to maintain the transmitted energy inside the RC, whereas the K-factor is the ratio between the direct and scattered energy [20], [27], [28]. The RC environment has been already used to test the 4G-LTE system [25], [29], [30], [31], [32], [33], [34], [35], [36].

In this paper, we present results of a measurements campaign executed in the RC of the Università Politecnica delle Marche, in cooperation with Telecom Italia and Nokia, focused on the mmWave frequency range.

II. SET-UP DESCRIPTION

The RC used in this measurement campaign has dimensions 4 m wide ($\hat{x}$), 6 m long ($\hat{y}$) and 2.5 m high ($\hat{z}$). It is large enough to hold antennas, UEs, absorbers and all instruments we need. The RC is equipped by two stirrers, a vertical Z-folded stirrer and a horizontal stirrer. Figure 1 shows the 2D schematic of the adopted set-up. During measurements, the vertical stirrer always remained stationary, while the horizontal stirrer rotated in continuous way in some tests. During tests we changed the antenna orientation: i) in "Pos1" it faces towards the RC door (highlighted in blue in Figure 1); ii) in "Pos2" it faces towards the RC horizontal stirrer (highlighted in red in Figure 1).

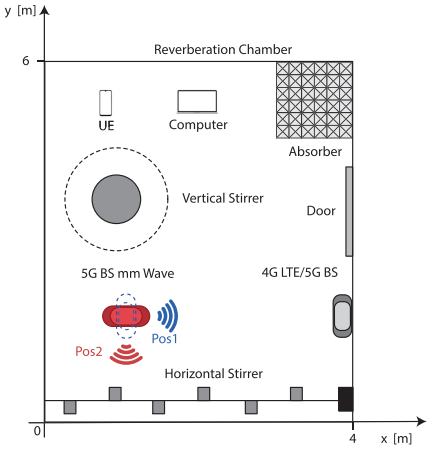

FIGURE 1. Schematic description of the set-up. During measurements we considered two antenna orientations labeled as "Pos1" and "Pos2" respectively.

In this measurement campaign we used a 5G Nokia BS, the Askey terminal and the QXDM software in order to collect data from the user point of view. Figure 2 shows the GPS antenna installed in our laboratory and the UE Askey

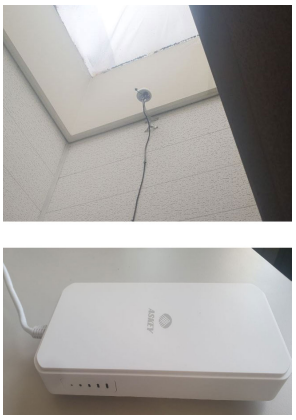

FIGURE 2. The top picture shows the GPS antenna used to synchronize the 5G pilot signal. The bottom picture reports the Askey UE used to collect data.

terminal. From the mobile operator point of view, Nokia operator is able to have direct access to BS data thanks to the BS manufacturer proprietary software. The radio modules, both 4G LTE and 5G, were connected to the TIM's live core network with an optical fiber. In this work two real life scenarios were emulated, more precisely a commercial (#1) and a residential (#2) ones. The time delay spread effectively quantifies the environment multipath propagation condition, as specified by ITU [37], [38]. In order to characterize the chamber we collected the S_{21} parameters by a VNA between two horn antennas. The investigated frequency range during these tests is from to 27 to 29 GHz. By performing an IFT we evaluated the chamber impulse response from

$$h(t) = \mathrm{IFT}[S_{21}]. \tag{1}$$

Then, the PDP is evaluated by

$$\mathrm{PDP}(t) = \left\langle |h(t)|^2 \right\rangle_N, \tag{2}$$

where $\langle\cdot\rangle$ denotes the ensemble average over the N stirrer positions. When the PDP is computed, a threshold were considered. This value defines the minimum signal level considered to compute the τ_{RMS}, we set the threshold equal to -20 dB [39], [40]. The time delay spread (τ) and its root mean square (τ_{RMS}) are related to the PDP and computed by eq. (3) and eq. (4) respectively.

$$\tau_{\mathrm{RMS}} = \frac{\sqrt{\int_0^\infty (t-\tau_{ave})^2\,\mathrm{PDP}(t)\,dt}}{\int_0^\infty \mathrm{PDP}(t)\,dt}, \tag{3}$$

$$\tau_{ave} = \frac{\int_0^\infty t\mathrm{PDP}(t)\,dt}{\int_0^\infty \mathrm{PDP}(t)\,dt}. \tag{4}$$

The Q-factor of the chamber conveys the ratio between the stored energy and the dissipated power within the RC and it is computed by

$$Q = \frac{16\pi^2 V \left\langle |S_{21}|^2 \right\rangle_N}{\eta_{TX}\eta_{RX}\lambda^3}, \tag{5}$$

where V is the volume of the RC, λ is the free-space wavelength, S_{21} are the scattering parameters and η_{TX}, η_{RX} are the transmitting and receiving antenna total efficiencies, respectively. By means of the Q-factor it is possible to evaluate the decay time of the chamber by [16]:

$$\tau = \frac{Q}{\omega}, \tag{6}$$

where ω denotes the angular frequency. The B_c is computed by the relationship:

$$B_c = \frac{f}{Q}, \tag{7}$$

where f denotes the frequency. Figure 3 shows the Q-factor of the explored scenarios. The chamber Q-factor rapidly reduces when absorbing materials is inserted. The final effect expected passing from "Scenario #1" to "Scenario #2" is a reduction in the energy inside the RC, giving the same transmitted power. Consequently, the signal level experienced by the UE will reduce. Figure 4 reports the coherence bandwidth. The B_c essentially is the band within which the propagation properties of the channel do no vary appreciably.

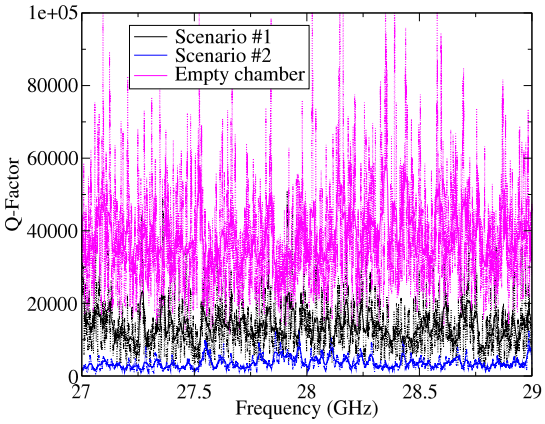

FIGURE 3. Quality factor for the different chamber loading condition, EC, ML and UHL. Dotted lines denotes raw data whereas continuous lines are the raw data are after by applying a sliding average in a window of 400 frequency points.

Explored chamber loading configurations are:

- EC: within the chamber there are only cables, PC, UE and the BS. In this case, the Q-factor is high, losses mechanism are offset by the high frequency range;
- ML chamber ("Scenario #1"): nine anechoic absorbing panels (Emerson & Cuming VHP-8-NRL) are added within the RC. The setup is reported in the top picture of Figure 5. The Q-factor decreases w.r.t. the EC case as showed in Figure 3. This load condition emulates a commercial scenario;
- UHL chamber ("Scenario #2"): in this scenario forty-five anechoic absorbing panels (Emerson & Cuming VHP-8-NRL), four anechoic absorbing panels (Emerson & Cuming VHP-18-NRL) and seven planar absorbing panels (Emerson & Cuming ANW-77) were

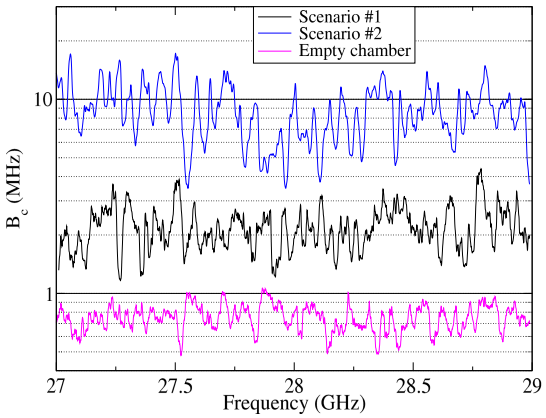

FIGURE 4. Coherence bandwidth.

placed on the RC floor and resting on wooden boards lean in the walls. The setup is reported in the bottom picture of Figure 5. In this situation the Q-factor decreases w.r.t the ML condition. This load condition emulates a residential scenario.

The more the chamber is loaded, the more the Q factor is reduced. Combinations of number and position of absorbers within the RC differently affect the overall loading behavior [25]. In this measurement campaign we arranged absorbing panels on the floor, on walls of the chamber and in a metallic organizer in order to control: i) the Q-factor, ii) the PDP and iii) τ_{RMS} [41], [42], [43]. We performed measurements at the mmWave frequency range, in this scenario the transmitted beam has a high directivity and this implies a narrow beam [44]. The RC exhibits a different behavior at mmWave w.r.t. sub-6 GHz analyzed in the past [25], [29], [30], [31], [32], [33], [34], [35], [36]. In this way, unless you want to block the direct connection, the position of the absorbing material is not so relevant in a multipath also considering that the signal after some reflections fades considerably. At the mmWave range the PDP fades more quickly than lower frequencies, i.e. sub-6 GHz [25], and that is precisely why new 5G systems use beamforming and high gain antennas that compensate the channel in hostile situations while maintaining a radio link acceptable. As we will see shortly, the 5G active smart antenna is able to select the best configuration, in terms of selected beam(s), to create and maintain the mobile connection.

In Figure 5 are reported the ML and UHL setup used during tests. In order to emulate a real-life scenario, the number of absorbing materials was progressively increased until the computed τ_{RMS} matched its value reported in the standard [37], [38]. The PDP of those scenarios are reported in Figure 6. In the UHL scenario the PDP exhibits a greater reduction w.r.t ML case. The PDP variation affects the τ_{RMS}, the computed values are reported in Table 1 considering a threshold of -20 dB [24]. The PDP reduction occurs for a larger interception of rays by absorbers before they reach the receiving antenna.

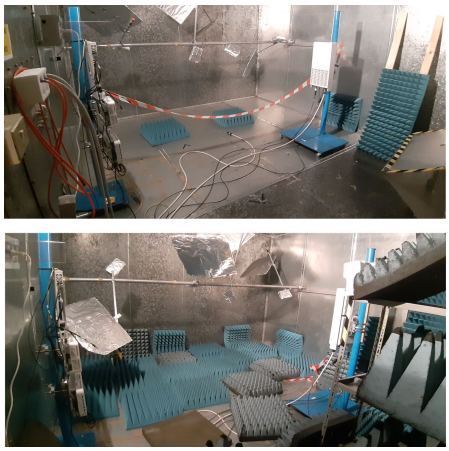

FIGURE 5. Inner view of the RC. On the top the ML condition whereas on the bottom the UHL condition. Moreover, for the antenna orientation the top picture denotes "Pos1" whereas the bottom picture refers to "Pos2".

TABLE 1. Time delay spread applying a threshold of -20 dB.

Frequency (GHz)	Environment	τ_{RMS} (ns)
28	#1: Commercial	65
28	#2: Residential	19

In Table 1 are reported the computed τ_{RMS}, its reduction occurs for a larger interception of rays by absorbers before they reach the receiving antenna.

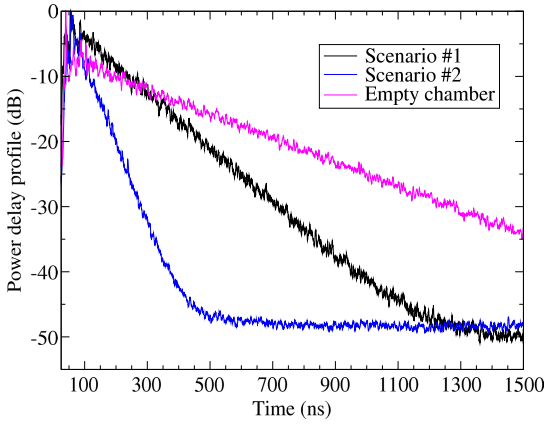

FIGURE 6. Power delay profile for different chamber loading condition.

III. BS OPERATING CONDITIONS

The AEUB Nokia active antenna architecture used in these measurements is no stand alone, it needs the control signal by the 4G LTE modules. Figure 7 shows the 5G and 4G LTE RF antenna modules. The mmWave antenna, the right one showed in Figure 7 has dimensions 603 mm height, 304 mm width and 124 mm thick. In spite of the transmitted power due to the control signal that lean on the LTE, it exhibits

a little impact in the UL scenario and it is negligible on the total transmitted power. The mmWave 5G antenna is configured by MIMO 2 × 2, with a bandwidth of 1 GHz and a maximum power of 28 dBm for each transmitter whereas the antenna gain is 28 dBi. The total average EIRP is 60 dBm. The supported operating frequency band are from 27.50 to 28.35 GHz and from 26.50 to 29.50 GHz. The operating center frequency in our tests was 26.95 GHz. The single SSB has maximum power of 16 dBm whereas the transmitted power of the UE is 23 dBm. During tests we enabled the carrier aggregation, in spite of we used only 1 cell. The MIMO 2 × 2 is present both in DL and UL. In these tests, the maximum attainable throughput is 550 Mbps for the DL and 140 Mbps in UL. The frame for both beamforming and broadcast is composed by 40 slots, each with a duration of 0.125 ms. In fact, every 0.5 ms the system sends 1 SSB and the terminal highlight which beam exhibits the best RSRP, then move on the throughput. The AEUB Nokia has an analog beamforming, no other techniques are implemented such as refining beam. The mobile operator can choose from multiple beam set configurations each of them has a different beam pattern. For preliminary tests we fix the 32 beams configuration reported in Figure 8, with one centered beam and the others on vertical panels. In this configuration, the beam set azimuth opening angle is from −60 deg to +60 deg whereas the elevation opening angle is from +87 deg to +123 deg.

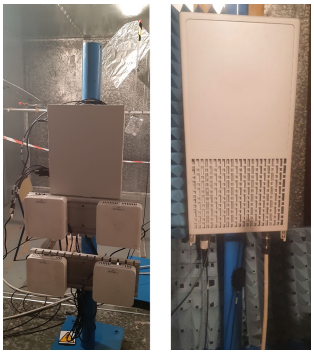

FIGURE 7. Pictures of the BS antennas. On the left, on the top the 5G antennas at 3.7 GHz whereas on the bottom the 4G LTE RF modules. On the right the 5G mmWave antenna with analog beamforming.

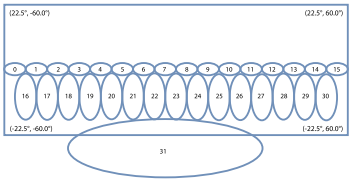

FIGURE 8. Selected pattern configuration of the 32 beams.

The envelope of all beams is showed in Figure 9, in accordance with what is shown in Figure 8. The radiation patterns are plotted by using a proprietary software provided by the BS vendor. It is also possible to choose and set only one beam for tests. It is worth noticing that in a real situation, if a beam points to an obstacle that intercepts the chosen beam, the antenna switches to the close beam. The distance between maximum and zeros of the radiation pattern is very small. In this context the overall gain remains high in order to maintain a high RSRP. This fact is opposite to the LTE scenario where the relocation of the receiver can cause an evident degradation in terms of RSRP.

The UE used to monitor the evaluation of the BS is an Askey RTL 6305, which has MIMO 2 × 2 in UL.

IV. RESULTS

In all tests, in every radio configuration (also when -60 dBm SSB), MIMO 2 × 2 were always maintained. It can be explained by the paths uncorrelation on the tested environments. The throughput reduction does not depend on the diversity scheme but it is due to the SNR degradation, both from DL and UL. Measured throughput values are reported in Table 2 for DL case whereas in Table 3 for UL case. The static case is identified by a stationary stirrer, labeled as "OFF" whereas rotating stirrer denotes the dynamic scenario labeled as "ON". The maximum throughput achievable is 550 Mbps when the MCS is about 28, related to a 64 QAM current modulation. The throughput is evaluated by the product of two factors, so resulting into a non-integer number:

- the ratio between DAI received in DL and the DL slot of their transmission;
- TDD frame, namely the ratio between the number of DL slot and total number of frame slot.

Moreover, the MCS value reported in our results is not an integer value because it is averaged over every acquisition time slot, i.e. every 0.125 ms. Both throughput and MCS are close to the maximum achievable. The beam serving distribution, are almost the same, in particular beam #3. For the UL scenario in all the explored cases, reported in Table 4, both RSRP and SINR are always good, probably due to the operation of beamforming.

In order to check the capability of the antenna beamforming to highlight the best transmission configuration, in "Pos1" case we covered the RC door by absorbing material, see Figure 10. The beam serving distribution changed and the selected beam from the BS is the beam #5 instead of beam #3, Figure 11 shows the beam switching. This behavior can be explained in that the preferable path is blocked by absorbing materials thus the BS select a beam that hits again the wall of the chamber, mitigating the effect of the added obstacle and maintaining the same quality of the communication. No evident changes in terms of RSRP are observed. This indirectly confirms the capability of the BS antenna to beamform the radiation pattern also inside the RC.

We also investigated the scenario when the RC door, covered by absorbing material, is opened. In this case we measured:

- DL: throughput 538.62 Mbps – MCS of 26.12 – 15 dB SINR – rank 2

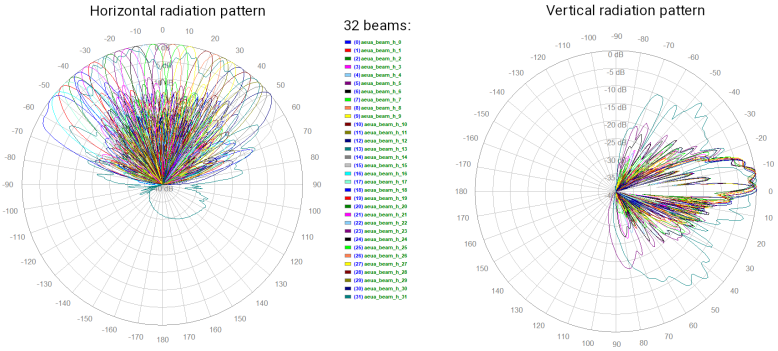

FIGURE 9. Radiation pattern of the 32 beams. The envelop of beams can cover from -60 deg to +60 deg azimuth angle.

FIGURE 10. Door of the RC covered by two VHP-18-NRL and one ANW-77 absorber.

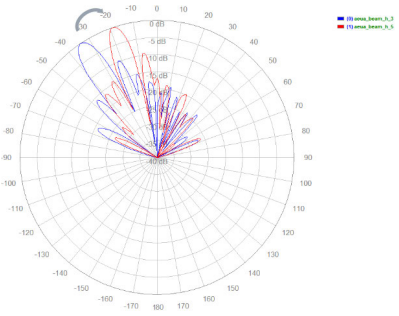

FIGURE 11. Horizontal radiation pattern when the door is blocked by absorbing panels in the "Pos1" case. The BS switches from beam#3 (blue) to beam#5 (red).

- UL: throughput 75.80 Mbps – MCS of 24.41 – 15.74 dB SINR – rank 2.

We are able to reduce the power broadcast but not the overall power, so it is not possible to degrade a lot the radio propagation. Up to −40 dBm there are no significant throughput variation. When the SSB block power is reduced to −60 dBm, differently the SINR measured by the UE (related to the SQI) decreased as well as the throughput, 259 Mbps, and the MCS of 17.88 w.r.t. MCS of 26 in previous case. No impact on MIMO distribution are observed.

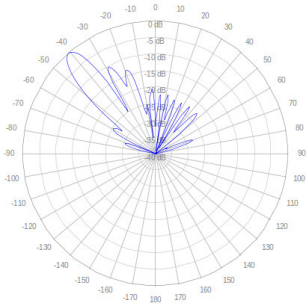

FIGURE 12. Horizontal radiation pattern of scenario #2, 5G antenna at "Pos2".

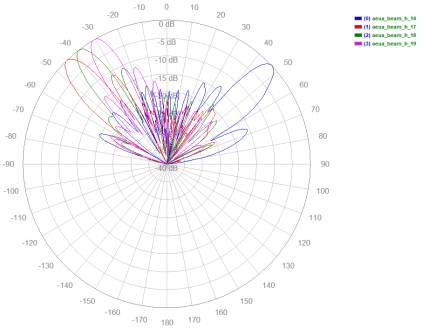

FIGURE 13. Horizontal radiation pattern of the selected beams for scenario #2, 5G antenna at "Pos2", and the RC door is covered by anechoic panels. In the label are reported the beams activated by the BS.

TABLE 2. GNB DL performance.

Position	Scenario	Stirrer	Throughput (Mbps)	MCS	Rank
1	#1	ON	532.74	25.65	2
1	#1	OFF	542.31	25.73	2
1	#2	ON	539.48	24.84	2
1	#2	OFF	330.88	20.71	2
2	#1	ON	536.31	24.41	2
2	#1	OFF	536.8	25.68	2
2	#2	ON	525.2	25.38	2
2	#2	OFF	506.65	25.24	2

TABLE 3. UE UL performance.

Position	Scenario	Stirrer	Throughput (Mbps)	MCS	Rank
1	#1	ON	100.19	26.3	2
1	#1	OFF	100.25	26.98	2
1	#2	ON	53.12	18.2	2
2	#2	OFF	65.41	16.5	2

TABLE 4. UE side: RSRP (dBm) and SNR (dB).

Position	Scenario	Stirrer	RSRP (dBm)	SNR (dB)
1	#1	OFF	-55.5	-6.7
1	#2	OFF	-56.8	-8.2
1	#1	ON	-55.9	-6.9
1	#2	ON	-57.2	-9.0
2	#1	OFF	-57.6	-7.5
2	#2	OFF	-59.1	-10.8
2	#1	ON	-58.1	-8.1
2	#2	ON	-59.8	-12.7

We also investigated the "Pos2" in two scenarios:

- the RC door was free;
- the RC door was covered with absorbing materials.

In the first case the BS activated always the same beam (−40 deg) to ensure a good connection, as shown in Figure 12. In the second case, in presence of absorbing material, the BS is compelled to switch the beam at different angles to ensure the connection, as shown in the radiation pattern reported in Figure 13. It seems that the variation of the B_c from "Scenario #1" to "Scenario #2" does not appreciably impact on results due to the larger bandwidth adopted by the BS, i.e. 100 MHz.

By comparing the throughput, RSRP and MCS reported in Tables 2, 3 and 4 respectively, it is evident that when the horizontal stirrer was rotating, it did not remarkably affect the quality of the transmission once the BS selected the optimal beam. This robustness against the stirrer rotation is evident in both DL and UL in combination of "Pos1", "Pos2", and in both investigated scenarios, i.e. "Scenario #1" and "Scenario #2". This can be carried to a commercial scenario, e.g a factory, where there are moving conductive objects, e.g. AVGs, that intercept the trajectory of the 5G signal for a while, like our stirrer acts.

V. CONCLUSION

As we are approaching the deployment of 5G systems in the mmWave range, we conducted an experimental analysis in this frequency range by means of commercial 5G devices such as BS, antenna and UE and thanks to the support from the mobile operator (TIM) and vendor (Nokia). In particular, this measurements campaign focused on the KPIs evaluation of a commercial 5G BS that operates at the mmWave frequency range, center frequency at 26.95 GHz. Measurements are performed in the university facility, i.e. the RC which allows us to emulate a residential and a commercial real-life environment. We investigated the capability of the BS system to exploit the propagation channel in which it operates. Main results of these measurements campaign show that RSRP, throughput, MCS and SINR collected by the UE and by BS are good and stable in the explored radio conditions. In our tests we evaluated the functionalities of the BS which is able to maintain a good communication link in the investigated scenarios. We showed that the BS scans the area and selects the beam, or more than one, for the transmission and it is able to change the beam in presence of link blockage. We forced the BS to change the beam in two ways. We can select the wanted beam of the BS antenna by means of a dedicated tool provided by the Nokia software which controls the entire BS functionalities. In the first way, we covered the RC door with absorbing materials. In fact, in one scenario just one beam was selected by the BS to ensure the connection with the UE but when the setup was altered by adding absorbing material in the region illuminated by the selected beam, the BS changed the selected beam. In the second way, we stressed the BS by continuously rotating the RC stirrer that acts as a conductive element which may change the boundary conditions of the environment. The BS is able to reconfigure itself by maintaining a good radio link connection, close to the maximum achievable, in case of whatever changes may occur in the surrounding environment. A key factor that explains the capability to maintain a good connection is the high gain of the antenna, about 28 dBi, and the possibility to swap across 32 beams. The MIMO is always used both in UL and DL direction. In the UL direction the UE does not achieve the maximum power, this aspect needs to be investigated if this behavior is due to the power control parameters or to thermal protection mechanism.

LIST OF ACRONYMS

Acronym	Full-form
2D	Two Dimensional.
4G LTE	Fourth Generation Long Term Evolution.
5G	Fifth Generation.
AVG	Automated Guided Vehicles.
B_c	Coherence Bandwidth.
BS	Base Station.
DAI	Downlink Assignment Index.
DL	Downlink.
eMBB	Enhanced Mobile Broadband.
EC	Empty Chamber.
EIRP	Effective Isotropic Radiated Power.
GNB	Next Generation Node B.
GPS	Global Positioning System.
IFT	Inverse Fourier Transform.
IoT	Internet of Things.
ITU	International Telecommunication Union.
KPI	Key Performance Indicator.
mmWave	millimeter-wave.
M2M	Machine-to-Machine.
MCS	Modulation Coding Scheme.
MIMO	Multiple-Input Multiple-Output.
ML	Medium Load.
OTA	Over the air Tests.
PDP	Power Delay Profile.

Q-factor	Quality factor.
QAM	Quadrature Amplitude Modulation.
QXDM	QUALCOMM eXtensible Diagnostic Monitor.
RC	Reverberation Chamber.
RF	Radio Frequency.
RIS	Reconfigurable Intelligent Surface.
RSRP	Reference Signals Received Power.
SINR	Signal to Interference plus Noise Ratio.
SNR	Signal to Noise Ratio.
SSB	Synchronization Signal Block.
SQI	Signal Quality Indicator.
TDD	Time Division Duplex.
UE	User Equipment.
UL	Uplink.
UHL	Ultra High Load Chamber.
VNA	Vector Network Analyzer.

ACKNOWLEDGMENT

This work was supported by the European Union (EU) HORIZON 2020 (H2020) Reconfigurable Intelligent Sustainable Environments for 6G Wireless Networks (RISE-6G) Project under Grant 101017011.

REFERENCES

[1] *IMT Vision—Framework and Overall Objectives of the Future Development of IMT for 2020 and Beyond*, ITU Recommendation, document M.2083-0, Sep. 2015.
[2] *Study on New Services and Markets Technology Enablers*, 3GPP, document TR22.891, Sep. 2016.
[3] A. Ghosh, A. Maeder, M. Baker, and D. Chandramouli, "5G evolution: A view on 5G cellular technology beyond 3GPP release 15," *IEEE Access*, vol. 7, pp. 127639–127651, 2019.
[4] K. Sakaguchi, G. K. Tran, H. Shimodaira, S. Nanba, T. Sakurai, K. Takinami, I. Siaud, E. C. Strinati, A. Capone, I. Karls, R. Arefi, and T. Haustein, "Millimeter-wave evolution for 5G cellular networks," *IEICE Trans. Commun.*, vol. 98, no. 3, pp. 388–402, Mar. 2015.
[5] V. Sciancalepore, K. Samdanis, X. Costa-Perez, D. Bega, M. Gramaglia, and A. Banchs, "Mobile traffic forecasting for maximizing 5G network slicing resource utilization," in *Proc. IEEE Conf. Comput. Commun.*, May 2017, pp. 1–9.
[6] *Ericsson Mobility Report*, ERICSSON, Stockholm, Sweden, Nov. 2021.
[7] E. Calvanese Strinati and S. Barbarossa, "6G networks: Beyond Shannon towards semantic and goal-oriented communications," *Comput. Netw.*, vol. 190, May 2021, Art. no. 107930.
[8] E. C. Strinati, G. C. Alexandropoulos, V. Sciancalepore, M. Di Renzo, H. Wymeersch, D.-T. Phan-Huy, M. Crozzoli, R. D'Errico, E. De Carvalho, P. Popovski, P. Di Lorenzo, L. Bastianelli, M. Belouar, J. E. Mascolo, G. Gradoni, S. Phang, G. Lerosey, and B. Denis, "Wireless environment as a service enabled by reconfigurable intelligent surfaces: The RISE-6G perspective," in *Proc. Joint Eur. Conf. Netw. Commun. 6G Summit*, Jun. 2021, pp. 562–567.
[9] G. C. Alexandropoulos, M. Crozzoli, D.-T. Phan-Huy, K. D. Katsanos, H. Wymeersch, P. Popovski, P. Ratajczak, Y. Bénédic, M.-H. Hamon, S. H. Gonzalez, R. D'Errico, and E. C. Strinati, "Smart wireless environments enabled by RISs: Deployment scenarios and two key challenges," in *Proc. Joint Eur. Conf. Netw. Commun. 6G Summit*, Jun. 2022, pp. 1–6.
[10] S. Adda, T. Aureli, S. D'Elia, D. Franci, E. Grillo, M. D. Migliore, S. Pavoncello, F. Schettino, and R. Suman, "A theoretical and experimental investigation on the measurement of the electromagnetic field level radiated by 5G base stations," *IEEE Access*, vol. 8, pp. 101448–101463, 2020.
[11] S. Adda, T. Aureli, S. Bastonero, S. D'Elia, D. Franci, E. Grillo, M. D. Migliore, N. Pasquino, S. Pavoncello, F. Schettino, A. Schiavoni, R. Scotti, R. Suman, and M. Vaccarono, "Methodology based on vector and scalar measurement of traffic channel power levels to assess maximum exposure to electromagnetic radiation generated by 5G NR systems," *IEEE Access*, vol. 10, pp. 12125–12136, 2022.
[12] K. Sakaguchi, T. Haustein, S. Barbarossa, E. Strinati, A. Clemente, G. Destino, A. Pärssinen, I. Kim, H. Chung, J. Kim, W. Keusgen, R. Weiler, K. Takinami, E. Ceci, A. Sadri, L. Xain, A. Maltsev, G. K. Tran, H. Ogawa, and R. Heath, "Where, when, and how mmWave is used in 5G and beyond," *IEICE Trans. Electron.*, vol. 100, no. 10, pp. 790–808, 2017.
[13] D. Choudhury, "5G wireless and millimeter wave technology evolution: An overview," in *IEEE MTT-S Int. Microw. Symp. Dig.*, May 2015, pp. 1–4.
[14] P. Corona, G. Latmiral, and E. Paolini, "Performance and analysis of a reverberating enclosure with variable geometry," *IEEE Trans. Electromagn. Compat.*, vol. EMC-22, no. 1, pp. 2–5, Feb. 1980.
[15] P.-S. Kildal, C. Orlenius, and J. Carlsson, "OTA testing in multipath of antennas and wireless devices with MIMO and OFDM," *Proc. IEEE*, vol. 100, no. 7, pp. 2145–2157, Jul. 2012.
[16] *Electromagnetic compatibility (EMC)—Part 4–21: Testing and Measurement Techniques—Reverberation Chamber Test Methods*, Standards IEC 61000-4-21, Geneva, Switzerland, Apr. 2011.
[17] Y. Ren, C. Pan, X. Yang, X. Zhang, and X. Wu, "Measurement of total radiated power in reverberation chamber for 5G millimeter wave base station," in *Proc. Int. Conf. Microw. Millim. Wave Technol. (ICMMT)*, May 2021, pp. 1–3.
[18] A. Gifuni, M. Adil, G. Grassini, A. Buono, F. Nunziata, D. Micheli, and M. Migliaccio, "An effective method using reverberation chambers to measure TRP from mobile phones and power absorbed by user body," *IEEE Trans. Electromagn. Compat.*, vol. 64, no. 4, pp. 951–962, Aug. 2022.
[19] F. Li, S. Huang, W. Xue, Y. Ren, and X. Chen, "Signal and coherence bandwidth effects on total radiated power measurements of LTE devices in reverberation chambers," *IEEE Trans. Instrum. Meas.*, vol. 71, pp. 1–3, 2022.
[20] C. L. Holloway, D. A. Hill, J. M. Ladbury, P. F. Wilson, G. Koepke, and J. Coder, "On the use of reverberation chambers to simulate a Rician radio environment for the testing of wireless devices," *IEEE Trans. Antennas Propag.*, vol. 54, no. 11, pp. 3167–3177, Nov. 2006.
[21] P. Corona, G. Ferrara, and M. Migliaccio, "Reverberating chambers as sources of stochastic electromagnetic fields," *IEEE Trans. Electromagn. Compat.*, vol. 38, no. 3, pp. 348–356, Aug. 1996.
[22] D. A. Hill, "Plane wave integral representation for fields in reverberation chambers," *IEEE Trans. Electromagn. Compat.*, vol. 40, no. 3, pp. 209–217, Aug. 1998.
[23] K. A. Remley, S. J. Floris, H. A. Shah, and C. L. Holloway, "Static and dynamic propagation-channel impairments in reverberation chambers," *IEEE Trans. Electromagn. Compat.*, vol. 53, no. 3, pp. 589–599, Aug. 2011.
[24] C. L. Holloway, H. A. Shah, R. J. Pirkl, K. A. Remley, D. A. Hill, and J. Ladbury, "Early time behavior in reverberation chambers and its effect on the relationships between coherence bandwidth, chamber decay time, RMS delay spread, and the chamber buildup time," *IEEE Trans. Electromagn. Compat.*, vol. 54, no. 4, pp. 714–725, Aug. 2012.
[25] L. Bastianelli, L. Giacometti, V. M. Primiani, and F. Moglie, "Effect of absorber number and positioning on the power delay profile of a reverberation chamber," in *Proc. IEEE Int. Symp. Electromagn. Compat. (EMC)*, Dresden, Germany, Aug. 2015, pp. 422–427.
[26] Z. Wang, Y. Ren, Y. Zhang, C. Pan, and X. Zhang, "A novel mode-stirred reverberation chamber design for 5G millimeter wave bands," *IEEE Access*, vol. 9, pp. 38826–38832, 2021.
[27] X. Chen, P. Kildal, and J. Carlsson, "Verification of the Rician K-factor-based uncertainty model for measurements in reverberation chambers," *IET Sci., Meas. Technol.*, vol. 9, no. 5, pp. 534–539, Aug. 2015, doi: 10.1049/iet-smt.2014.0344.
[28] C. Lemoine, E. Amador, and P. Besnier, "Mode-stirring efficiency of reverberation chambers based on Rician K-factor," *Electron. Lett.*, vol. 47, no. 20, p. 1114, 2011.
[29] D. Micheli, M. Barazzetta, C. Carlini, R. Diamanti, V. M. Primiani, and F. Moglie, "Testing of the carrier aggregation mode for a live LTE base station in reverberation chamber," *IEEE Trans. Veh. Technol.*, vol. 66, no. 4, pp. 3024–3033, Apr. 2017.
[30] D. Micheli, M. Barazzetta, F. Moglie, and V. M. Primiani, "Power boosting and compensation during OTA testing of a real 4G LTE base station in reverberation chamber," *IEEE Trans. Electromagn. Compat.*, vol. 57, no. 4, pp. 623–634, Aug. 2015.
[31] M. Barazzetta, D. Micheli, L. Bastianelli, R. Diamanti, M. Totta, P. Obino, R. Lattanzi, F. Moglie, and V. M. Primiani, "A comparison between different reception diversity schemes of a 4G-LTE base station in reverberation chamber: A deployment in a live cellular network," *IEEE Trans. Electromagn. Compat.*, vol. 59, no. 6, pp. 2029–2037, Dec. 2017.

[32] D. Micheli, M. Barazzetta, R. Diamanti, P. Obino, R. Lattanzi, L. Bastianelli, V. M. Primiani, and F. Moglie, "Over-the-air tests of high-speed moving LTE users in a reverberation chamber," *IEEE Trans. Veh. Technol.*, vol. 67, no. 5, pp. 4340–4349, May 2018.
[33] L. Bastianelli, G. Gradoni, D. Micheli, M. Barazzetta, R. Diamanti, F. Moglie, and V. M. Primiani, "Reverberation chambers for testing LTE wireless communication systems," in *Proc. Int. Conf. Electromagn. Adv. Appl. (ICEAA)*, Sep. 2017, pp. 722–725.
[34] D. Micheli, M. Barazzetta, L. Bastianelli, R. Diamanti, C. Carlini, M. Colombo, F. Moglie, and V. Mariani Primiani, "MIMO 4×4 vs. MIMO 2×2 performance assessment of a real life LTE base station in a reverberation chamber," *AEU-Int. J. Electron. Commun.*, vol. 129, Feb. 2021, Art. no. 153500. [Online]. Available: https://www.sciencedirect.com/science/article/pii/S1434841120311973
[35] M. Barazzetta, M. Colombo, L. Bastianelli, F. Moglie, V. M. Primiani, R. Diamanti, and D. Micheli, "Testing of VoLTE mean opinion score in reverberation chambers," *IET Sci., Meas. Technol.*, vol. 14, no. 8, pp. 949–954, Oct. 2020, doi: 10.1049/iet-smt.2019.0385.
[36] M. Barazzetta, D. Michel, R. Diamanti, L. Bastianelli, F. Moglie, and V. M. Primiani, "Optimization of 4G wireless access network features by using reverberation chambers: Application to high-speed train LTE users," in *Proc. 46th Eur. Microw. Conf. (EuMC)*, Oct. 2016, pp. 719–722.
[37] *Guidelines for Evaluation of Radio Interface Technologies for IMT—Advanced*, document M.2135-1, ITU, Dec. 2009.
[38] *Propagation Data and Prediction Methods for the Planning of Indoor Radiocommunication Systems and Radio Local Area Networks in the Frequency Range 900 MHz to 100 GHz*, document P.1238-7, ITU Recommendation, Feb. 2012.
[39] E. Genender, C. L. Holloway, K. A. Remley, J. M. Ladbury, G. Koepke, and H. Garbe, "Simulating the multipath channel with a reverberation chamber: Application to bit error rate measurements," *IEEE Trans. Electromagn. Compat.*, vol. 52, no. 4, pp. 766–777, Nov. 2010.
[40] *Studies for Short-Path Propagation Data and Models for Terrestrial Radiocommunication Systems in the Frequency Range 6 GHz to 100 GHz*, document P.2406-0, ITU Report, Sep. 2017.
[41] C. L. Holloway, M. G. Cotton, and P. McKenna, "A model for predicting the power delay profile characteristics inside a room," *IEEE Trans. Veh. Technol.*, vol. 48, no. 4, pp. 1110–1120, Jul. 1999.
[42] E. Genender, C. L. Holloway, K. A. Remley, J. Ladbury, G. Koepke, and H. Garbe, "Use of reverberation chamber to simulate the power delay profile of a wireless environment," in *Proc. Int. Symp. Electromagn. Compat.*, Sep. 2008, pp. 1–6.
[43] H. Fielitz, K. A. Remley, C. L. Holloway, Q. Zhang, Q. Wu, and D. W. Matolak, "Reverberation-chamber test environment for outdoor urban wireless propagation studies," *IEEE Antennas Wireless Propag. Lett.*, vol. 9, pp. 52–56, 2010.
[44] C. A. Balanis, *Antenna Theory: Analysis and Design*. Hoboken, NJ, USA: Wiley, 2005.

MICHELE COLOMBO received the M.Sc. degree in electronic engineering from Politecnico di Milano, Milan, Italy, in 1998. He is currently with the Department of Network Performance and Optimization, Nokia Networks Italia, Rome. He is involved in radio access design, optimization, and testing for UMTS, LTE, and 5G technologies.

RICCARDO DIAMANTI received the degrees in telecommunications engineering and electronics engineering from the University of Ancona (now Università Politecnica delle Marche), Ancona, Italy, in 2000 and 2015, respectively. He is currently a Specialist in network performance management with Telecom Italia (TIM S.p.A).

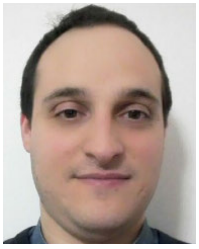

LUCA BASTIANELLI (Member, IEEE) received the M.S. degree in electronic engineering and the Ph.D. degree in biomedical, electronics and telecommunication engineering from Università Politecnica delle Marche, Ancona, Italy, in 2014 and 2018, respectively. During the Ph.D. degree, he spent seven months with the University of Nottingham, Nottingham, U.K.

In 2018, he was a Research Fellow with the Dipartimento di Ingegneria dell'Informazione, Università Politecnica delle Marche. He is currently a Researcher with the CNIT, Dipartimento di Ingegneria dell'Informazione, Università Politecnica delle Marche. He is involved in the area of electromagnetic compatibility, telecommunications, and computational electrodynamics. He was involved in many PRACE projects. He currently leads the FDTDLIME project on reconfigurable intelligent surfaces and the H2020 RISE-6G project. His research interests include reverberation chambers, wave chaos, propagation in complex systems, ray tracing, time reversal, metasurfaces, 5G, and numerical techniques on high-performance computers. He was a member of the Cost Action IC1407 ACCREDIT. He is an active member of the Working Group for the development of the IEEE Standards P2718 on near-field characterization. He received the URSI Commission E Young Scientist Award, in 2017. During the fellowship, he is involved in teaching support activities.

GABRIELE GRADONI (Member, IEEE) received the Ph.D. degree in electromagnetics from Università Politecnica delle Marche, Ancona, Italy, in 2010. He was a Visiting Researcher with the Time, Quantum, and Electromagnetics Team, National Physical Laboratory, Teddington, U.K., in 2008. From 2010 to 2013, he was a Research Associate with the Institute for Research in Electronics and Applied Physics, University of Maryland, College Park, MD, USA. From 2013 to 2016, he was a Research Fellow with the School of Mathematical Sciences, University of Nottingham, U.K., where he was a Full Professor of mathematics and electrical engineering. Since June 2020, he has been an Adjunct Associate Professor with the Department of Electrical and Computer Engineering, University of Illinois at Urbana–Champaign, Champaign, IL, USA. Since 2020, he has been a Royal Society Industry Fellow with British Telecom, U.K. Since December 2022, he has been a Visiting Fellow with the Department of Computer Science and Technology, University of Cambridge, U.K. Since May 2023, he has been a Full Professor and the Chair of Wireless Communications with the 6G Innovation Centre, Institute for Communication Systems, University of Surrey, Guildford, U.K. His research interests include probabilistic and asymptotic methods for propagation in complex wave systems, metasurface modeling, quantum/wave chaos, and quantum computational electromagnetics, with applications to electromagnetic compatibility and modern wireless communication systems. He is a member of the Italian Electromagnetics Society. He received the URSI Commission B. Young Scientist Award, in 2010 and 2016, the Italian Electromagnetics Society Gaetano Latmiral Prize, in 2015, and the Honorable Mention IEEE TEMC Richard B. Schulz Transactions Prize Paper Award, in 2020. From 2014 to 2021, he was the URSI Commission E. Early Career Representative.

EMANUEL COLELLA received the B.Sc. and master's (cum laude) degrees in biomedical engineering from Università Politecnica delle Marche, in 2015 and 2019, respectively, where he is currently pursuing the Ph.D. degree in electromagnetics, with a focus on electromagnetic analysis of complex structures using classical and quantum algorithms. In 2020, he was with CNIT as a Researcher for the RISE-6G project. He worked on computational electrodynamic simulations of RIS to analyze their performance in a smart radio environment. In 2022, he was designated as the project lead of working group P2718 on the characterization of unintentional stochastic radiators.

VALTER MARIANI PRIMIANI (Senior Member, IEEE) received the Laurea degree (summa cum laude) in electronic engineering from the University of Ancona, Ancona, Italy, in 1990.

He is currently an Associate Professor in electromagnetic compatibility (EMC) with Università Politecnica delle Marche, Ancona. He is also a member of the Department of Information Engineering, where he is responsible for the EMC Laboratory. Since 2003, he has been involved in research activities on the application of reverberation chambers for compliance testing, metrology applications, and multipath propagation emulation. He has also been a member of the COST Action 1407 ACCREDIT on the characterization of stochastic emissions from digital equipment. Since 2021, he has been involved in the RISE–6G project. His research interests include the prediction of digital printed circuit board radiation, the radiation from apertures, the electrostatic discharge coupling effects modeling, and the analysis of emission and immunity test methods.

Prof. Primiani is a Senior Member of the IEEE (EMC Society) and a member of the Italian Society of Electromagnetics. From 2007 to 2013, he was an active member of some working groups for the development of IEEE Standards: 299.1-2013 on shielding effectiveness measurements. Since 2014, he has been a member of the International Steering Committee of EMC Europe. He is currently an Associate Editor of the *IET Science, Measurement and Technology* journal.

FRANCO MOGLIE (Senior Member, IEEE) received the "Dottore Ingegnere" degree in electronics engineering from the University of Ancona, Ancona, Italy, in 1986, and the Ph.D. degree in electronics engineering and electromagnetics from the University of Bari, Bari, Italy, in 1992.

Since 1986, he has been a Research Scientist with Università Politecnica delle Marche, Ancona, where he has been an Associate Professor, since 2016. Since 2007, he has been a member of the "Accademia Marchigiana di Scienze, Lettere ed Arti–Istituto Culturale Europeo" (Marches Academy of Sciences, Arts and Letters–European Cultural Institute), which is based in Ancona. In 2011, he was a Visiting Researcher with the Wave Chaos Group, IREAP, University of Maryland, College Park, MD, USA. Since 2011, he has been with the Department of Information Engineering, Università Politecnica delle Marche. From 2013 to 2019, he led three PRACE high-performance computing projects on reverberation chambers. His current research interest includes EM numerical techniques. In particular, his research activity is in the field of the application of reverberation chambers for compliance testing, metrology applications, and multipath propagation.

Prof. Moglie is a member of the IEEE Electromagnetic Compatibility Society and the Italian Electromagnetics Society. Since 2007, he has been an active member of some working groups for the development of IEEE Standards, such as 299.1, 1302, 2715, and 2716. Since 2014, he has been an Italian Management Committing Member of the COST Action IC1407. Since 2017, he has been a Secretary of the working group for the IEEE Standard 2718. Since 2021, he has been the Scientific Manager of CNIT, Università Politecnica delle Marche, in the RISE–6G project. In 2013, he received the title of Distinguished Reviewer of IEEE TRANSACTIONS ON ELECTROMAGNETIC COMPATIBILITY.

DAVIDE MICHELI received the "Dottore Ingegnere" degree in electronics engineering from the University of Ancona (now the Università Politecnica delle Marche), Ancona, in 2001, and the master's degree in astronautic engineering and the Ph.D. degree in aerospace engineering from the "Sapienza" University of Rome, Rome, Italy, in 2007 and 2011, respectively.

He is currently with the Department of Wireless Access Engineering, Telecom Italia (TIM S.p.A.), Rome, Italy. He is involved in 2G, 3G, 4G, and 5G radio access network parameterization and optimization.